PHYSICAL REVIEW B VOLUME 22, NUMBER 6 15 SEPTEMBER 1980

# Surface structure of ZnTe (110) as determined from dynamical analysis of low-energy-electron diffraction intensities

R. J. Meyer, C. B. Duke, and A. Paton
*Xerox Webster Research Center, Xerox Square-W114, Rochester, New York 14644*

E. So, J. L. Yeh, A. Kahn, and P. Mark*
*Department of Electrical Engineering, Princeton University, Princeton, New Jersey 08540*
(Received 29 January 1980)

Dynamical calculations of the intensities of normally incident low-energy electrons diffracted from ZnTe (110), performed using a matrix-inversion method, are compared for structures resulting from (i) a kinematical search, (ii) a dynamical search, and (iii) energy-minimization calculations. Second-layer structural distortions as well as top-layer reconstructions are examined in our structural search. Our analysis leads to the selection of the most probable surface structure for ZnTe (110) as one in which the top layer Te moves outward 0.20 Å and the top layer Zn moves inward 0.55 Å, corresponding to a surface bond angle of 33.2°. No convincing evidence is obtained for second-layer reconstruction. The structure is different from zinc-blende (110) surface structures previously examined, e.g., GaAs (110) and InSb (110), in that the in-plane anion displacement in the surface layer is only half that characteristic of a rigid bond rotation, and the second atomic layer beneath the surface appears to be undistorted to within the accuracy of our analysis. The difference between ZnTe and more covalent zinc-blende materials is attributed to a dependence of the structure of (110) surfaces of zinc-blende-compound semiconductors on the bulk bonding ionicity.

## I. INTRODUCTION

Atomic geometries for the (110) surfaces of zinc-blende–structure compound semiconductors have been extracted via analyses of several spectroscopic measurements, including elastic low-energy-electron-diffraction (ELEED) intensities,[1-12] angular integrated ultraviolet photoemission spectra (UPS),[9,13,14] angle-resolved ultraviolet-photoemission spectra (ARUPS),[15-17] polarization-dependent angle-resolved photoemission spectra (PARUPS),[16,18] and the electron paramagnetic resonances (EPR) of adsorbed $O_2$ species.[19] Moreover, three procedures for determining these atomic geometries via minimization of surface energy functionals have been proposed.[19-22] It has been demonstrated that for GaAs (110) all of these methodologies lead to compatible surface structures within their inherent uncertainties.[23,11] In addition to the quite thorough treatment of GaAs (110), fragmentary spectroscopic results are available for the (110) surfaces of ZnSe,[3,24] GaP,[19,25] and AlSb.[19] A preliminary report of the work described herein for ZnTe (110) appeared earlier,[12] and a complete ELEED intensity analysis for InSb (110) recently has been given[26,27] although no photoemission studies of that surface have yet been reported. Finally, energy-minimization predictions have been published for the (110) surfaces of ZnSe,[21] GaP,[20] AlSb,[20] ZnTe,[21,28] InP,[21] and InSb.[21]

The purpose of this paper is to address several issues which have arisen during the course of the earlier analyses noted above. First and foremost, we report a dynamical ELEED structural analysis for the (110) face of a new material, ZnTe. Our analysis is comparable in both technique and comprehensiveness to those of GaAs (110) (Refs. 1, 2, 10, and 11) and InSb (110) (Refs. 26 and 27) reported earlier, and removes an ambiguity between two different types of surface structure which could not be resolved by the previous preliminary (less-extensive) examination of ZnTe (110) (Ref. 12). Second, we focus our attention on the two central structural issues which emerged from the earlier structural analyses: the distinction between bond-rotation[1,2,10,11] and bond-relaxation[6-8,11] geometries of the surface layer and the occurrence of subsurface atomic relaxations. Third, we investigate the compatibility between the range of surface structures consistent with the ELEED intensity analysis and the predictions of energy-minimization calculations. Fourth and finally, because some of our results for the structure of ZnTe (110) are unanticipated, we reexamine the proposed relationships[2] between the surface structures of compound semiconductors and their bulk bonding ionicity.

Our main results reported herein are the extension of our earlier kinematical and dynamical ELEED intensity profile analysis[12] through a completely dynamical structure search, and the utilization of this search to establish a range of probable surface structures for ZnTe (110). We show via comparison of theoretical model intensity pro-

 

files with data gathered for 14 beams that the structure of ZnTe (110) differs from those of GaAs (110) and InSb (110) in that (i) the surface bond angle, found to be 33.2°, is distinctly larger than the $25.6° \leq \omega \leq 28.8°$ range found for GaAs and InSb, (ii) no second or third layer distortions are found to occur, and (iii) the dominant bond-length change is a three percent contraction of the surface-cation–surface-anion bond, while the back bond between the surface anion and the second layer cation expands slightly. We also find that the structures determined by energy minimization[21,28] are not included within the conventional uncertainties of our best fit structure due to their predictions of large (~0.2 Å) subsurface shears.

Another important result documented by this paper is an explicit examination of the sensitivity of LEED to motions of surface species parallel to the surface. For GaAs (110) both "bond-relaxation"[16] (or "normal-displacement"[11]) models and "rotational-relaxation"[11] (or "bond-rotation"[11]) models have been considered.[10,11,16,19,20] Although, for GaAs (110), the bond-rotated structures appear to be superior to the normal-displacement ones, this important conclusion has generally been displayed in the literature only in terms of structures differing both in perpendicular and parallel atomic positions.[10,11,16] In this paper, we demonstrate the sensitivity of dynamical calculations of LEED intensities to atomic displacements parallel to the surface by comparing structures differing only in these coordinates. We will find for ZnTe (110), in contrast to GaAs (110) and InSb (110), a structure intermediate between the bond-rotated and the normal-displacement models is preferred.

We proceed as follows: In Sec. II we summarize our experimental procedure. In Sec. III we describe the nature of our ELEED intensity calculations. In Sec. IV we discuss the structure analysis, as well as the sensitivity of the calculated intensity profiles to atomic motions parallel to the surface. In Sec. V we summarize our findings and discuss their physical significance.

## II. EXPERIMENTAL PROCEDURES

The ZnTe sample was purchased from General Diode Corporation. While it is sufficiently conductive that sample charging did not occur, its doping is unknown. It was cut by the supplier, chemically polished at RCA using a proprietary etch, mounted in Mo foil, and sputter cleaned by 1-keV Ar ion bombardment for 10 min followed by a thermal anneal at $T = 808$ K for 50 min. Auger electron spectroscopy (AES) revealed that following this treatment the surface was clean and stochiometric to within the accuracy of the AES technique.

The low-temperature ELEED intensities reported herein were measured using a modified Physical Electronics Industries S/N-504-6-174 manipulator. Cooling was accomplished via a small liquid-nitrogen reservoir connected to the Mo foil in which the sample was mounted.

The ELEED intensities were obtained using a Physical Electronics Industries LEED system and a Gamma Scientific spot photometer to measure the intensities from the LEED display screen. Normal incidence was ensured by the symmetry of the spot pattern (see Fig. 1). ELEED intensity data were acquired for the [01], [0$\bar{1}$], [10]=[$\bar{1}$0], [11]=[$\bar{1}\bar{1}$], [1$\bar{1}$]=[$\bar{1}$1], [02], [0$\bar{2}$], [20]=[$\bar{2}$0], [21]=[$\bar{2}\bar{1}$], [12]=[$\bar{1}$2], [2$\bar{1}$]=[$\bar{2}$1], [1$\bar{2}$]=[$\bar{1}$2], [13]=[$\bar{1}$3], and [1$\bar{3}$]=[$\bar{1}\bar{3}$] beams as averages of three repeated runs for each intensity profile. The dimensions of the spot pattern revealed no significant deviation of the surface unit mesh from that expected of a truncated bulk crystal described by the geometrical

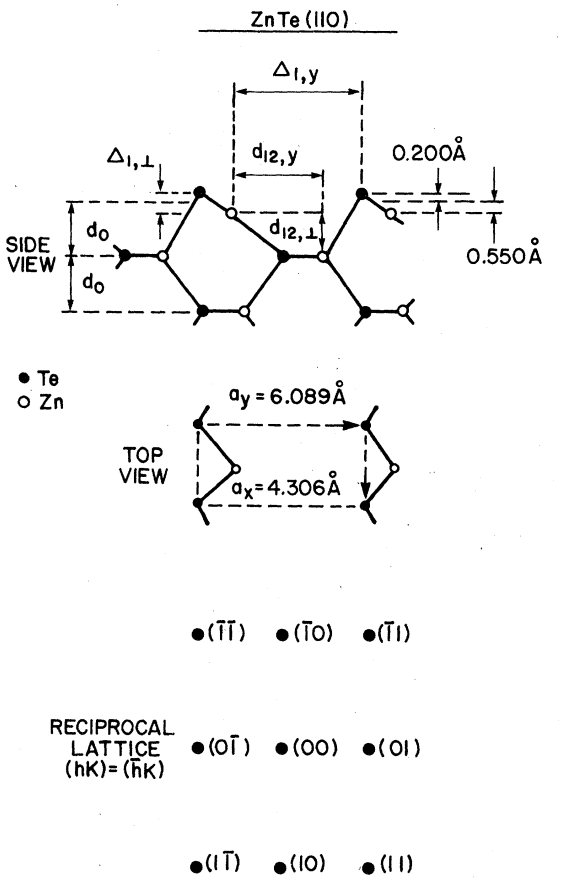


FIG. 1. Schematic indication of the surface atomic geometry and the associated ELEED normal-incidence spot pattern for the (110) surface of ZnTe. The symbols utilized in Table I are defined in the upper panel of the figure. The dimensions of the surface unit mesh are taken from Wyckoff's bulk structure (Ref. 29).

parameters given by Wyckoff[29] ($a_x = 4.306$ Å, $a_y = 6.089$ Å as indicated in Fig. 1).

## III. MODEL CALCULATIONS

An approximate multiple-scattering model of the diffraction process, described previously,[11] was used to calculate the ELEED intensities. The surface electron-ion core interaction was described by a one-electron muffin-tin potential. The electron-electron interaction is incorporated via an optical potential represented by a complex function with constant real part $V_0$ and an imaginary part characterized by the inelastic collision mean free path $\lambda_{ee}$.[30] By trial and error we have chosen $V_0 = 4$ eV and $\lambda_{ee} = 8$ Å.

The one-electron crystal potential is formed from a superposition of overlapping ionic (e.g., $Zn^+Te^-$) charge densities.[31] The local Slater approximation[32] is used for the exchange potential. The bulk crystal structure (see Fig. 1) is that given by Wyckoff.[29] We use the muffin-tin radii $r_{MT}^{Zn} = 1.22$ Å, $r_{MT}^{Te} = 1.42$ Å, as determined from crystal potential crossover. The Wigner-Seitz radii are $r_{WS}^{Zn} = 1.74$ Å and $r_{WS}^{Te} = 2.02$ Å. Once the crystal potential in a given Wigner-Seitz cell has been obtained, it is reduced to muffin-tin form. The resulting phase shifts are shown in Fig. 2.

In view of the problems entailed in correctly including bulk lattice vibrations in diatomic systems[33] we have calculated our structures using a rigid-lattice model for comparison with data taken at $T = 150$ K, where the effects of lattice vibrations are modest. The effects of surface lattice vibrations on the analysis of ELEED from GaAs (110) have been examined in some detail previously,[11] and will not be reexamined here.

In the approximate multiple-scattering model of the diffraction process used in the surface structure determination, the $T$ matrix for the top three bilayers was solved exactly, utilizing six phase shifts for both the Te and Zn species, while in the lower layers the $T$ matrix was approximated by the single-bilayer scattering amplitude.[11] To check the convergence of this approximation, for structure (g) in Table I we have performed a similar calculation solving, however, the $T$ matrix for the top four bilayers exactly. The results are presented in Fig. 3 for the [10] and [11] beams. As we see, the principal features of these beams are well reproduced in the three-layer-exact calculations [panels (a) and (c)], although some of the finer structure changes on going to four-layers exact [panels (b) and (d)]. Thus, given the reproducibility of ELEED data from compound semiconductors, our calculations in which the $T$ matrix for the top three layers is solved exactly is judged

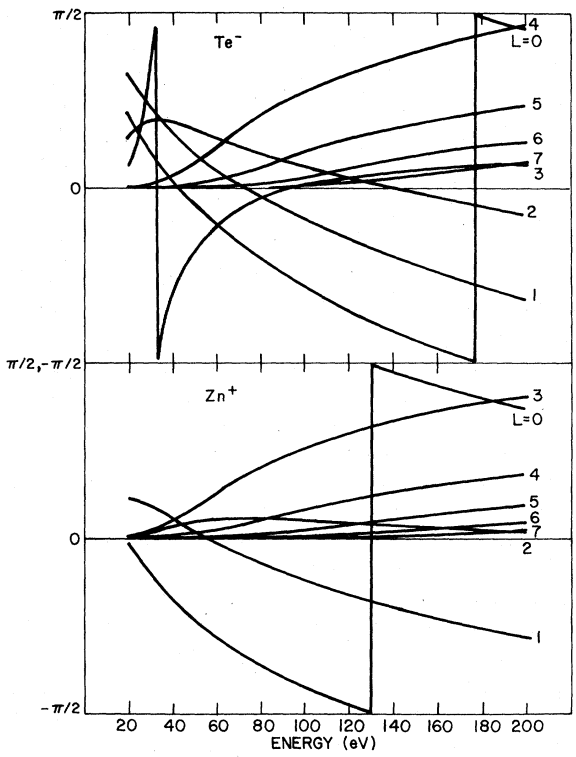


FIG. 2. Phase shifts for the $Zn^+$ and $Te^-$ species resulting from Slater exchange and the muffin-tin parameters described in Sec. III in the text.

to be adequate for the determination of surface structures to within an accuracy of 0.1 Å. Similarly, we have compared beam intensity profiles calculated using six phase shifts with those calculated using eight phase shifts for both Zn and Te species and have found little difference. Hence, six phase shifts are used in all of our calculations presented here.

## IV. STRUCTURAL ANALYSIS

As mentioned in the Introduction, in our preliminary study of ZnTe (110) (Ref. 12) two structures were found to be comparably compatible with measured ELEED intensities: a structure with a 0.4-Å top layer vertical shear and a 0.3-Å second layer shear, and a structure with a 0.8-Å first layer shear and no second-layer reconstruction. These structures were determined by a kinematical structure search in which comparisons with experimental data for five beams, the [01], $[0\bar{1}]$, [10]=$[\bar{1}0]$, [11]=$[\bar{1}1]$, and $[1\bar{1}]=[\bar{1}\bar{1}]$ beams, were performed. To resolve this ambiguity, we report here a new structural analysis which represents an expansion of our earlier work in four directions. First, as discussed in Sec. II, we have increased our data base from five to fourteen beams, including some beams out to third order.

TABLE I. Positions of the atoms in the uppermost three atomic bilayers for those reconstructed surfaces of ZnTe (110) for which calculated ELEED intensities are shown in Figs. 5–18. The symbols defining the structures are defined in the uppermost panel of Fig. 1. All distances are given in Angstroms.

| Structure | Layer | Te | Zn | $\Delta_{1,\perp}$ | $\Delta_{2,\perp}$ | $\Delta_{3,\perp}$ | $d_{12,\perp}$ | $d_{23,\perp}$ | $\Delta_{1,y}$ | $d_{12,y}$ | $\omega_1$ | $Zn_1-Te_1$ (% bond-length change) | $Zn_1-Te_2$ (% bond-length change) | $Te_1-Zn_2$ (% bond-length change) |
|---|---|---|---|---|---|---|---|---|---|---|---|---|---|---|
| (a) | 1 | +0.100 | +0.650 | | | | | | | | | | | |
| So | 2 | 0.0 | 0.0 | 0.750 | 0.0 | 0.0 | 1.503 | 2.153 | 5.126 | 3.604 | 37.92° | −6.13 | −2.61 | 3.12 |
| "Ionic" | 3 | 0.0 | 0.0 | | | | | | | | | | | |
| (Ref. 34) | | | | | | | | | | | | | | |
| (b) | 1 | +0.065 | +0.635 | | | | | | | | | | | |
| Chadi II | 2 | +0.065 | +0.108 | 0.700 | 0.173 | 0.0 | 1.410 | 2.261 | 4.803 | 3.318 | 28.56° | −1.25 | −9.20 | −2.14 |
| (Ref. 28) | 3 | 0.0 | 0.0 | | | | | | | | | | | |
| (c) | 1 | +0.200 | +0.550 | | | | | | | | | | | |
| Our best | 2 | 0.0 | 0.0 | 0.750 | 0.0 | 0.0 | 1.603 | 2.153 | 4.945 | 3.604 | 33.25° | −3.25 | −0.34 | 2.72 |
| | 3 | 0.0 | 0.0 | | | | | | | | | | | |
| (d) | 1 | +0.200 | +0.550 | | | | | | | | | | | |
| Our best | 2 | +0.07 | +0.100 | 0.750 | 0.170 | 0.0 | 1.503 | 2.253 | 4.945 | 3.604 | 33.25° | −3.25 | 1.30 | −0.56 |
| & 2nd layer | 3 | 0.0 | 0.0 | | | | | | | | | | | |
| (e) | 1 | +0.067 | +0.607 | | | | | | | | | | | |
| Chadi I | 2 | +0.086 | +0.114 | 0.674 | 0.200 | 0.065 | 1.432 | 2.310 | 4.796 | 3.388 | 27.53° | −1.36 | −6.00 | −3.93 |
| (Ref. 21) | 3 | +0.022 | +0.043 | | | | | | | | | | | |
| (f) | 1 | +0.215 | +0.535 | | | | | | | | | | | |
| Rigid | 2 | 0.0 | 0.0 | 0.750 | 0.0 | 0.0 | 1.617 | 2.153 | 4.764 | 3.604 | 29.59° | 0.00 | 0.00 | 0.00 |
| rotation | 3 | 0.0 | 0.0 | | | | | | | | | | | |
| (g) | 1 | +0.200 | +0.550 | | | | | | | | | | | |
| | 2 | 0.00 | +0.100 | 0.750 | 0.100 | 0.00 | 1.503 | 2.253 | 4.945 | 3.604 | 33.25° | −3.25 | −0.34 | −0.56 |
| Used in | 3 | 0.0 | 0.0 | | | | | | | | | | | |
| Fig. 3 | | | | | | | | | | | | | | |

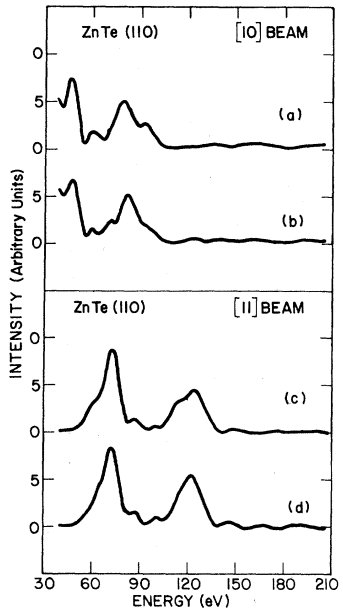


FIG. 3. Comparison of the predicted normal-incidence intensities for the [10] and [11] beams calculated using Slater exchange and a rigid lattice, with the surface given by panel (g) in Table I. Curve (a): calculated intensity of the [10] beam using six phase shifts and solving the $T$ matrix of the top three layers exactly. Curve (b), same as curve (a), but solving the $T$ matrix of the top four layers exactly. Curve (c), calculated intensity of the [11] beam using six phase shifts and solving the $T$ matrix of the top three layers exactly. Curve (d), same as curve (c), but solving the $T$ matrix of the top four layers exactly.

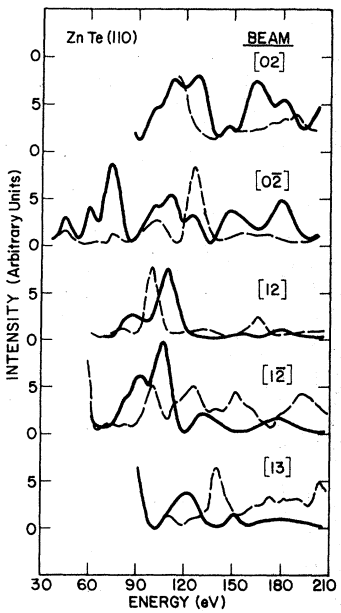


FIG. 4. Comparison of the calculated (solid curves: rigid lattice; six phase shifts) and measured (dashed curves) intensities for the [02], [0$\bar{2}$], [12], [1$\bar{2}$], and [13] diffracted beams for a structure with $\Delta_{1,\perp}=0.405$ Å, $\Delta_{2,\perp}=0.300$ Å as in Ref. 12, Table I, with the $y$ displacement appropriate for a 15.4° rigid-bond rotation.

Second, our present structure analysis, comprising approximately forty model structures, has been carried out utilizing dynamical ELEED intensity calculations. Third, the effect of atomic motions parallel to the surface have been investigated in detail. It is found that neither the "normal-displacement model" nor the "rotationally relaxed" (i.e., no bond length changes in the first layer) model gives the best correspondence with experiment but, rather, the best fit structures lie in a region of parameters which are intermediate between the two. Fourth, we have considered a new energy-minimized structure recently proposed for ZnTe (110) (Ref. 27) in response to the analysis reported in Ref. 12.

Dynamical calculations of our two-layer reconstruction[12] with a top layer shear of 0.4 Å and a second layer shear of 0.3 Å revealed this structure was incompatible with the larger data base of 14 beams. This is illustrated for the [02], [0$\bar{2}$], [12], [1$\bar{2}$], and [13] beams in Fig. 4. As a result, this region of parameter space was not explored further.

The earlier kinematical analysis[12] indicated acceptable agreement with experiment was obtained by raising the Te in the uppermost layer 0.15 ±0.1 Å and lowering the Zn in the uppermost layer 0.65 ±0.1 Å, producing a surface shear of 0.80 Å. Subsurface atoms remained at their bulk positions. Extensions of this early kinematical search[34] indicated, however, that a better structure was obtained by raising the top Te only 0.10 Å while leaving the surface Zn at 0.65 Å, producing a slightly smaller surface shear of 0.75 Å. This structure is contained within the uncertainties associated with the earlier structure. Dynamical investigation of this structure indicated improvement over the normal-displacement structure was obtained by moving the surface Zn atom 0.56 Å sideways, in the direction given by a rotation of the top bond forcing the Te outward. The resulting structure [see Table I, panel (a)] gave better comparison between theory and experiment than the earlier[12] 0.80 Å surface shear model, but yielded unsatisfactory correspondence between the two for several beams [e.g., see Figs. 9, 10, and 13, panel (a)].

Similarly, the published energy-minimized structure of Chadi[21] [see Table I, panel (e)] gave poor agreement with the measured intensities for the [1$\bar{1}$] [see Fig. 9, panel (e)], the [02] [see Fig. 10, panel (e)], and the [2$\bar{1}$] [see Fig. 14, panel (e)] beams. In response to earlier indications[12] of

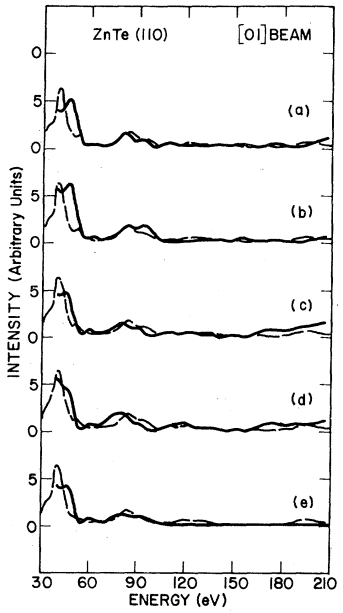


FIG. 5. Comparison of the calculated (solid curves, six phase shifts) and measured (dashed curves) intensities of the [01] beam of normally incident electrons diffracted from ZnTe (110). Curve (a): the measured intensity at $T=125$ K (dashed curve) and the calculated intensity (solid curve) using the bulk geometry of Wyckoff (Ref. 29) and the single layer "ionic" reconstruction of So (Ref. 34) described in panel (a) of Table I for a rigid-lattice model. Curve (b): same as curve (a), but evaluated using the two-layer structure of Chadi (Ref. 28) shown in panel (b) of Table I, and a rigid lattice. Curve (c): same as curve (a) but evaluated using the single-layer "best-fit" reconstruction described in Table I [panel (c)] and a rigid lattice. Curve (d): same as curve (c), but evaluated using the two-layer structure described in Table I [panel (d)] and a rigid lattice. Curve (e): same as curve (a), but evaluated using the three-layer reconstruction of Chadi (Ref. 21) described in Table I [panel (e)] and a rigid lattice.

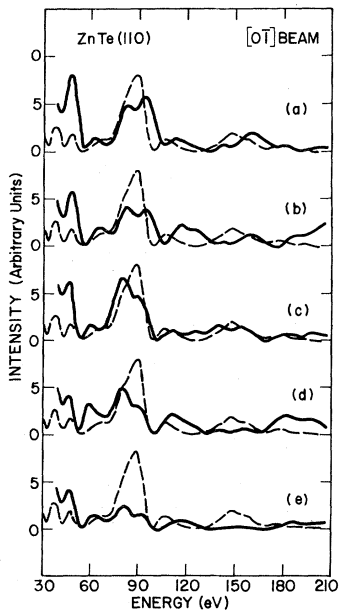


FIG. 6. Same as Fig. 5, only for the [0$\bar{1}$] beam.

this fact, however, a refined energy-minimized structure has been proposed for ZnTe (110) by Chadi[28] [see Table I, panel (b); Figs. 5–18, panel (b)]. This new structure has a slightly larger first layer shear of 0.70 Å, compared to the earlier value of 0.67 Å. The new structure, however, gave poor agreement with experiment for the [11] [see Fig. 8, panel (b)], the [0$\bar{1}$] [see Fig. 6, panel (b)], the [1$\bar{1}$] [see Fig. 9, panel (b)], the [20] [see Fig. 12, panel (b)], and [1$\bar{3}$] [see Fig. 18, panel (b)] beams. On balance, neither of the energy-minimized structures provide as good a description of the experimental intensities as that determined by the kinematical analysis [panel (a), Table I]. Hence we believe that a first layer shear of 0.75 Å, intermediate between the earlier kinematical result of 0.80 Å (Ref. 12) and the energy-minimized results of 0.67 Å (Ref. 21) and 0.70 Å (Ref. 28) yields the best comparison with experiment. This is especially so for the [11] (see Fig. 8), [11] [see Fig. 9], [02] (see Fig. 10), [02] (see Fig. 11), [12] (see Fig. 15), [1$\bar{2}$] (see Fig. 16), and [13] (see Fig. 17) beams.

In the kinematical best fit structure [Table I, panel (a)] the top bilayer-substrate distance is characterized by a value of $d_{12,\perp}=1.503$ Å. The

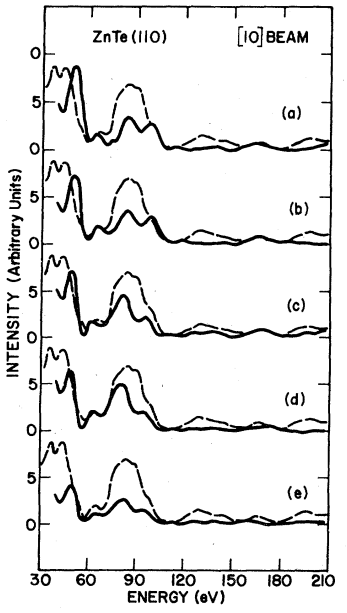


FIG. 7. Same as Fig. 5, only for the [10] beam.

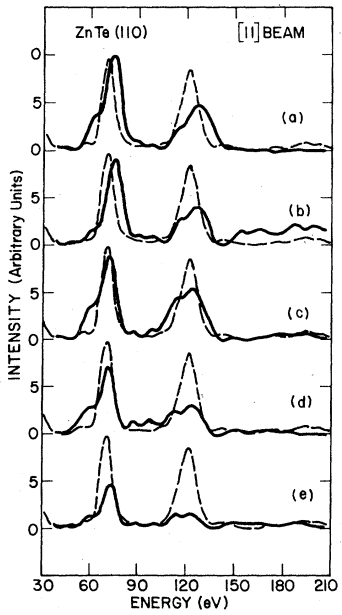


FIG. 8. Same as Fig. 5, only for the [11] beam.

"rotationally relaxed" structure, however, with surface shear 0.75 Å and bond angle $\omega_1 = 29.6°$ [see Table I, panel (f)] is characterized by a value $d_{12,\perp} = 1.617$ Å. In view of this discrepancy of 0.114 Å, we have dynamically investigated the top bilayer-substrate distance $d_{12,\perp}$. The optimum dynamically-determined surface bilayer-substrate distance of $d_{12,\perp} = 1.603$ [see Table I, panel (c) and Figs. 5–18, panel (c)] is equivalent to the rotationally relaxed value within the limits of ELEED precision.

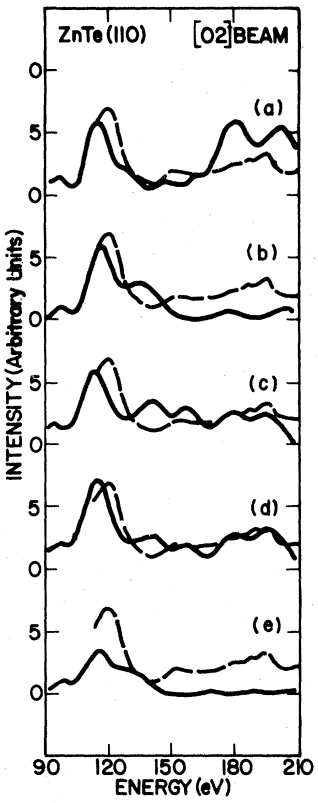


FIG. 10. Same as Fig. 5, only for the [02] beam.

Recent dynamical ELEED calculations for GaAs (110) (Ref. 11) and InSb (Refs. 26, 27) have shown

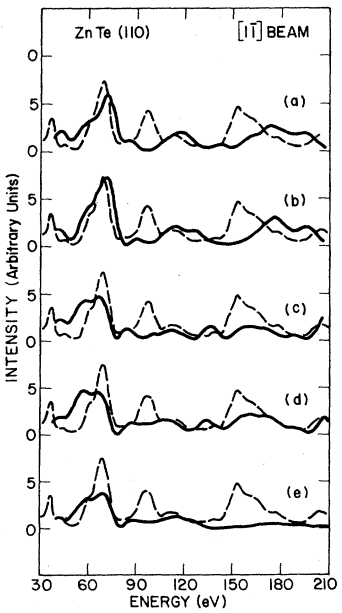


FIG. 9. Same as Fig. 5, only for the [1$\bar{1}$] beam.

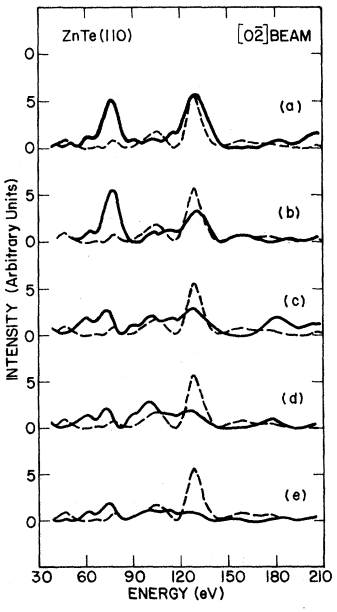


FIG. 11. Same as Fig. 5, only for the [0$\bar{2}$] beam.

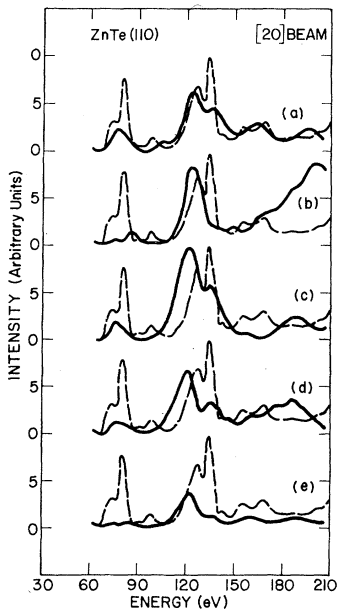


FIG. 12. Same as Fig. 5, only for the [20] beam.

that "rotationally relaxed" structures are superior to "normal-displacement" structures. As mentioned above, our best fit structure has the vertical spacings essentially equivalent to those of the

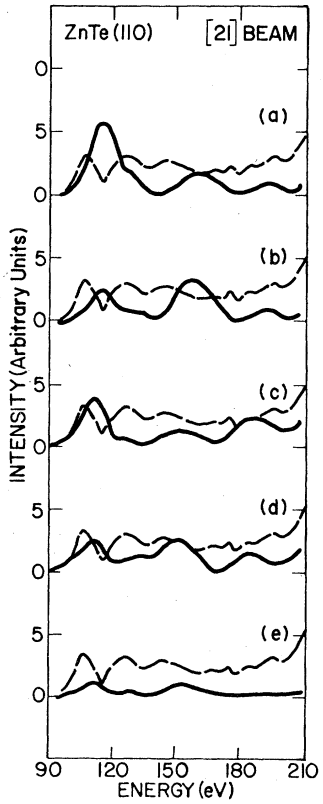


FIG. 13. Same as Fig. 5, only for the [21] beam.

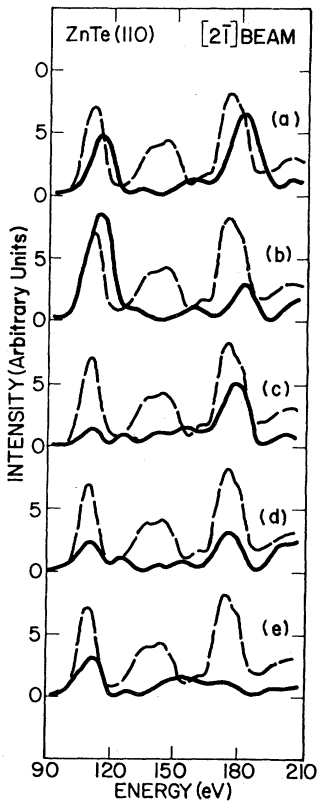


FIG. 14. Same as Fig. 5, only for the [2$\bar{1}$] beam.

"rotationally relaxed" structure. In order to check the applicability of our earlier conclusions on in-surface atomic displacements to ZnTe (110) we examined the $y$ motions of both surface Zn and Te

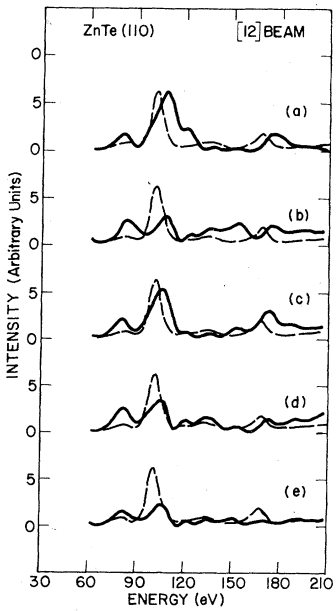


FIG. 15. Same as Fig. 5, only for the [12] beam.

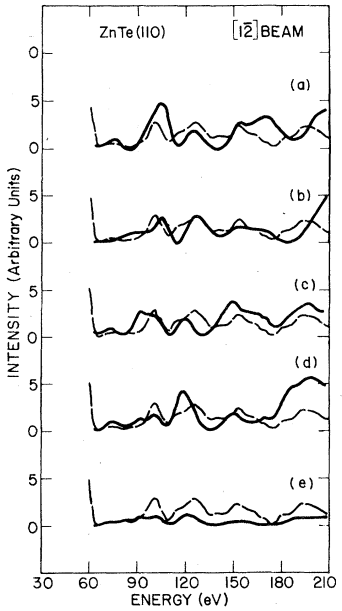


FIG. 16. Same as Fig. 5, only for the [1$\bar{2}$] beam.

species. Our optimum structure [Table I, panel (c)] has the same value of $d_{12,y}$ (see Fig. 1) as the corresponding rotationally relaxed structure [Table I, panel (f)], indicating that the surface

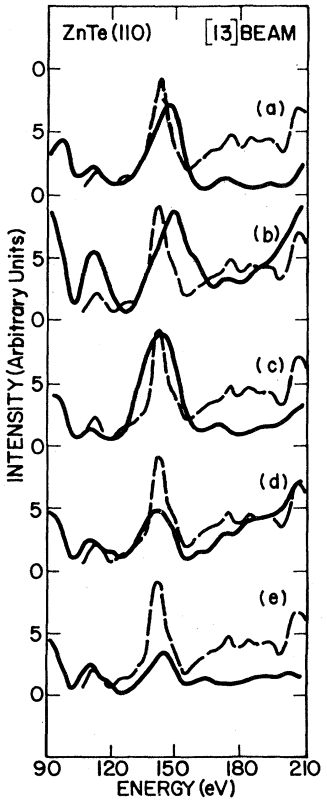


FIG. 17. Same as Fig. 5, only for the [13] beam.

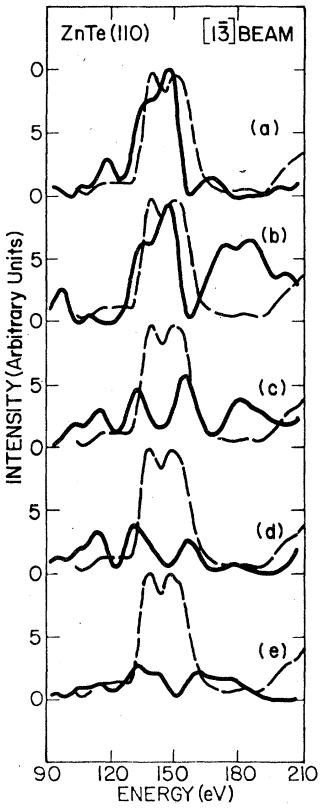


FIG. 18. Same as Fig. 5, only for the [1$\bar{3}$] beam.

Zn "rotates" just as we expect on the basis of studies of other zinc-blende (110) surfaces.[11,26,27] The sensitivity of our best fit structure to the surface Zn $y$ motion is indicated in Fig. 19 for the [20] and [1$\bar{3}$] beams. From the [20] beam we see the 120–150 eV experimental structure is best reproduced with a value of $d_{12,y}=3.804$ Å [Fig. 19, panel (a)], while $d_{12,y}=3.604$ Å [Fig. 19, panel (b)] is acceptable, and smaller values are clearly worse. From the [1$\bar{3}$] beam we see the 130–160 eV experimental structure is best described by a value of $d_{12,y}=3.604$ Å [Fig. 19, panel (e)], while both smaller and larger values are clearly inferior. Thus, we see that rotationally relaxed Zn $y$ motions (with $d_{12,y}=3.604$) yield best overall agreement with experiment, a conclusion which is supported through studies of intensity profiles for other beams.

The optimum Te $y$ motion relative to its bulk position, characterized in Table I [panel (c)] by $\Delta_{1,y}=4.945$ Å, is 0.181 Å smaller than that for the corresponding rotationally relaxed structure [Table I, panel (f)], and is halfway between those for the rotationally relaxed structure [Table I, panel (f)] and the structure with only Zn $y$ motion [Table I, panel (a)]. Thus, the Te sits halfway between its normal-displacement position and its

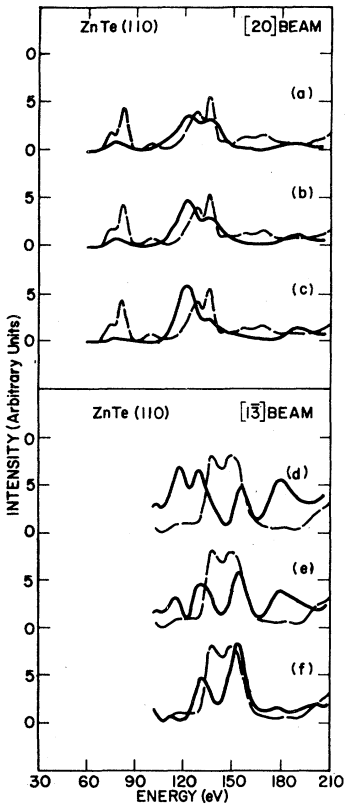


FIG. 19. Comparison of calculated (solid curves, six phase shifts, rigid lattice) and measured (dashed curves) intensities of the [20] and [1$\bar{3}$] beams of normally incident electrons diffracted from ZnTe (110) showing the effects of surface Zn parallel displacement. Curve (a): the measured [20] beam intensity at $T = 125$ K (dashed curve) and the calculated intensity (solid curve) using the bulk geometry of Wyckoff (Ref. 29) and the single-layer "best-fit" reconstruction described in Table I [panel (c)] except $d_{12,y} = 3.804$ Å and $\Delta_{1,y} = 5.145$ Å. Curve (b): same as curve (a), but evaluated using the "best fit" structure of Table I [panel (c)]. Curve (c): same as curve (a), but evaluated using $d_{12,y} = 3.404$ Å and $\Delta_{1,y} = 4.745$ Å. Curve (d): same as curve (a), but evaluated for the [1$\bar{3}$] beam. Curve (e): same as curve (b) but evaluated for the [1$\bar{3}$] beam. Curve (f): same as curve (c), but evaluated for the [1$\bar{3}$] beam.

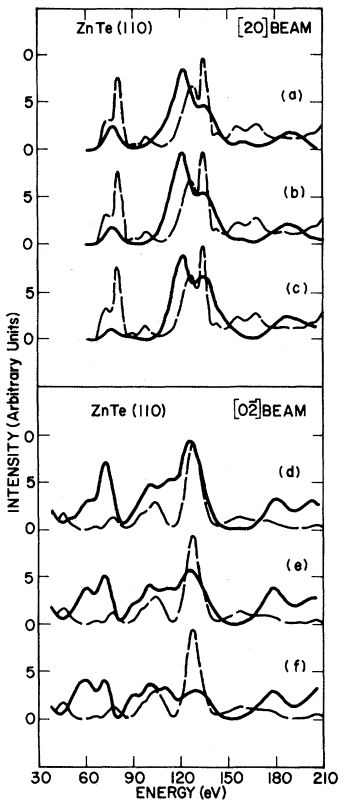


FIG. 20. Comparison of calculated (solid curves, six phase shifts, rigid lattice) and measured (dashed curves) intensities of the [20] and [0$\bar{2}$] beams of normally incident electrons diffracted from ZnTe (110) showing the effects of surface Te parallel displacements. Curve (a): the measured [20] beam intensity at $T = 125$ K (dashed curve) and the calculated intensity (solid curve) using the bulk geometry of Wyckoff (Ref. 29) and the single-layer "best-fit" reconstruction described in Table I [panel (c)] except $\Delta_{1,y} = 5.126$ Å. Curve (b): same as curve (a) except for the "best-fit" structure of Table I [panel (c)] i.e. $\Delta_{1,y} = 4.945$ Å. Curve (c): same as curve (a) except evaluated for $\Delta_{1,y} = 4.764$ Å. Curve (d): same as curve (a), but evaluated for the [0$\bar{2}$] beam. Curve (e): same as curve (b), but evaluated for the [0$\bar{2}$] beam. Curve (f): same as curve (c), but evaluated for the [0$\bar{2}$] beam.

rotationally relaxed position. The validity of this claim is indicated for the [20] and [0$\bar{2}$] beams in Fig. 20. For the [20] beam the 120–140 eV experimental structure is best reproduced by a structure [see Fig. 20, panel (c)] with rotated Te $y$ position, while the intermediate [Fig. 20, panel (b)] and normal displacement are inferior, but still acceptable. For the [0$\bar{2}$] beam the 60–140 eV structure is best described by the structure with normal displacement Te $y$ position [Fig. 20, panel (d)], while increasing the Te $y$ motion decreases the correspondence with experiment. Thus, the best overall agreement is obtained with the intermediate $y$ position of the surface Te atom.

Dynamical ELEED analyses of GaAs (110) (Ref. 11) and InSb (110) (Refs. 26 and 27) structures have indicated the presence of structural distortions extending at least two bilayers into the bulk. Energy-minimization calculations for ZnTe (110) (Refs. 21 and 28) [see e.g., Table I, panels (b) and (e)] also indicate the presence of subsurface reconstructions. In our dynamical ELEED analysis of ZnTe (110) we have searched for improvement in the comparison between theory and experiment resulting from second layer shears $\Delta_{2,\perp}$ in

the range $-0.02 < \Delta_{2\perp} < 0.2$ Å (i.e., shears in both directions). The best results for virtually all beams were obtained for little or no second layer shear [see Table I, panel (c)]. Previous dynamical analyses of zinc-blende (110) structures indicated that the [01], [$1\bar{1}$], and [21] beams were the most sensitive to second layer distortions.[11,26] In the present analysis the [01] [see Fig. 5, panels (c) and (d)], [21] [see Fig. 13, panels (c) and (d)] and [$1\bar{1}$] [see Fig. 9, panels (c) and (d)] beams are found to be insensitive to this variable. The only beams improved by subsurface distortions, the [$2\bar{1}$] [see Fig. 14, panels (c) and (d)] and the [$1\bar{3}$] [see Fig. 18, panels (c) and (d)] beams are more than offset by those worsened, e.g., see the [11] [see Fig. 8, panels (c) and (d)], [$0\bar{1}$] [see Fig. 6, panels (c) and (d)], and the [13] [see Fig. 17, panels (c) and (d)].

It is noteworthy that most of these structures, shown in Table I deviate from each other, in the vertical displacements, by less than the usually quoted[5,9,10] accuracy of ELEED structure analyses, i.e., $\Delta d_\perp < 0.1$ Å. Therefore, the significant structural results emanating from the dynamical multilayer analysis are the absence of second layer reconstructions, and the superiority of Te $y$ motion intermediate between those of the normal displacement and rotationally relaxed models.

## V. DISCUSSION

In this paper we report a surface structure determination for ZnTe (110) via dynamical ELEED analysis which represents an expansion of our earlier work in four directions. First, we have increased our data base from five to fourteen beams. Second, our present structure analysis has been completely carried out utilizing dynamical ELEED intensity calculations although our best-fit structure closely corresponds to one found kinematically. Third, the effect of both Zn and Te displacements parallel to the surface have been explored in detail. It is found that neither the "normal-displacement" model nor the "rotationally relaxed" model gives the best correspondence with experiment. Rather, in the case of ZnTe (110) the surface Zn atom is displaced parallel to the surface the usual amount for a rigid-bond rotation, while the surface Te atom has a reduced $y$ displacement. Fourth, we have considered two energy-minimized structures, one published and one recently proposed for ZnTe (110) (Ref. 28).

On the basis of our model calculations we conclude that only the uppermost atomic bilayer is reconstructed relative to the truncated bulk-solid structure[29] given by a unit mesh $a_x = 4.306$ Å, $a_y = 6.089$ Å, and atomic positions $d_{1,12} = 2.153$ Å, $d_{\perp,23} = 2.153$ Å, $\Delta_{y,1}(\mathrm{Zn}) = 4.567$ Å relative to a tellurium species at the origin of the unit mesh. Specifically, we find that $d_{\perp,12}(\mathrm{Te}) = 2.35 \pm 0.1$ Å, $d_{\perp,23}(\mathrm{Te}) = 2.153 \pm 0.1$ Å, $d_{\perp,12}(\mathrm{Zn}) = 1.603 \pm 0.1$ Å, $d_{\perp,23}(\mathrm{Zn}) = 2.153 \pm 0.1$ Å, and $\Delta_{1y}(\mathrm{Zn}) = 4.945 \pm 0.2$ Å. These tolerances, for practical purposes, exclude both of the energy-minimized structures proposed for ZnTe (110) by Chadi,[21,28] but include a 29.6° rigid-bond-rotation structure [see Table I, panel (f)]. There is no dynamical ELEED evidence indicating the presence of second or third layer structural distortions.

The single-layer reconstruction we have found for ZnTe (110); a $33.2° \pm 4.0°$ surface bond angle with the dominant bond length change a 3% contraction of the surface Zn–Te bond, is quite different from the final two-layer reconstructions found from dynamical ELEED analysis for GaAs (110) (Ref. 11) and InSb (110) (Ref. 26 and 27) and is more similar to the 34.8° single-layer reconstruction first proposed for GaAs (110) by Lubinsky *et al.*[1]

This difference in surface behavior between ZnTe (110) and GaAs (110) and InSb (110) is not surprising considering their large difference in Phillips ionicity.[35] In the Phillip's scale, GaAs and InSb have ionicities $f_i$ equal to 0.310 and 0.321, respectively. Hence we expect identical behavior for these materials. Estimates of the Phillips ionicity for ZnTe, however, vary from 0.49[36] to 0.61.[37] Thus ZnTe is roughly twice as ionic as the previously studied materials. (Indeed, ZnTe has ionicity near the maximum allowed, $f_i^{\mathrm{critical}} = 0.785 \pm 0.01$, for a zinc-blende material. For greater ionicity only rock salt structures occur.[35]) The ionicity of ZnTe is more similar to that of ZnO, with $f_i = 0.62$.[35-37] The surface reconstructions of ZnTe (110) and ZnO ($10\bar{1}0$) are also similar in that both are limited to the top atomic bilayer.[2,38-41] Thus, ionicity may be able to induce different surface structures on materials with identical bulk structures, as suggested by Duke *et al.*[2] in their "ionic reconstruction" model. Further ELEED analysis of ionic zinc-blende (110) surfaces are necessary to clearly resolve this question, although it is evident from the analysis reported above that the surface structure of ZnTe (110) is distinctly different in character from the corresponding structures of the covalent compound semiconductors GaAs and InSb.

## ACKNOWLEDGMENTS

The authors are indebted to L. Kennedy for assistance and to M. D. Tabak for generous support

of this work. Supported in part by the office of Naval Research (Grant No. N00014-75-G0394), Army Research (Grant No. CDAAG 29-77-G-0116), the National Science Foundation (Grant No. NSF-ENG 75-18529), and the Mobil Oil Foundation.

---

*Deceased.

[1]A. R. Lubinsky, C. B. Duke, B. W. Lee, and P. Mark, Phys. Rev. Lett. 36, 1058, 1058 (1976).
[2]C. B. Duke, A. R. Lubinsky, B. W. Lee, and P. Mark, J. Vac. Sci. Technol. 13, 761 (1976).
[3]C. B. Duke, A. R. Lubinsky, M. Bonn, G. Cisneros, and P. Mark, J. Vac. Sci. Technol. 14, 294 (1977).
[4]C. B. Duke, J. Vac. Sci. Technol. 14, 870 (1977).
[5]P. Mark, G. Cisneros, M. Bonn, A. Kahn, C. B. Duke, A. Paton, and A. R. Lubinsky, J. Vac. Sci. Technol. 14, 910 (1977).
[6]A. Kahn, G. Cisneros, M. Bonn, P. Mark, and C. B. Duke, Surf. Sci. 71, 387 (1978).
[7]A. Kahn, E. So, P. Mark and C. B. Duke, J. Vac. Sci. Technol. 15, 580 (1978).
[8]A. Kahn, E. So, P. Mark, C. B. Duke, and R. J. Meyer, J. Vac. Sci. Technol. 15, 1223 (1978).
[9]C. B. Duke, Crit. Rev. Solid State Sci. 8, 69 (1978).
[10]S. Y. Tong, A. R. Lubinsky, B. J. Mrstik, and M. A. Van Hove, Phys. Rev. B 17, 3303 (1978).
[11]R. J. Meyer, C. B. Duke, A. Paton, A. Kahn, E. So, J. L. Yeh, and P. Mark, Phys. Rev. B 19, 5194 (1979).
[12]C. B. Duke, R. J. Meyer, A. Paton, P. Mark, E. So, and J. L. Yeh, J. Vac. Sci. Technol. 16, 647 (1979).
[13]K. C. Pandey, J. L. Freeouf, and D. E. Eastman, J. Vac. Sci. Technol. 14, 904 (1977).
[14]K. C. Pandey, J. Vac. Sci. Technol. 15, 440 (1978).
[15]J. A. Knapp, D. E. Eastman, K. C. Pandey, and F. Patella, J. Vac. Sci. Technol. 15, 1252 (1978).
[16]D. J. Chadi, J. Vac. Sci. Technol. 15, 631 (1978); 15, 1244 (1978); Phys. Rev. B 18, 1800 (1978).
[17]A. Huijser, J. Van Laar, and T. L. Van Rooy, Phys. Rev. Lett. 65A, 337 (1978).
[18]G. P. Williams, R. J. Smith, and G. J. Lapeyre, J. Vac. Sci. Technol. 15, 1249 (1978).
[19]D. J. Miller and D. Haneman, J. Vac. Sci. Technol. 15, 1267 (1978).
[20]D. J. Miller and D. Haneman, Surf. Sci. 82, 102 (1979).
[21]D. J. Chadi, Phys. Rev. Lett. 41, 1062 (1978); Phys. Rev. B 19, 2074 (1979).
[22]W. A. Goddard III, J. J. Barton, A. Redondo, and T. C. McGill, J. Vac. Sci. Technol. 15, 1274 (1978).
[23]C. B. Duke, R. J. Meyer, A. Paton, P. Mark, A. Kahn, E. So, and J. L. Yeh, J. Vac. Sci. Technol. 16, 647 (1979).
[24]C. Calandra, F. Manghi, and C. M. Bertoni, J. Phys. C: Solid State Phys. 10, 1911 (1977).
[25]C. M. Bertoni, O. Bisi, F. Maghi, and C. Calandra, J. Vac. Sci. Technol. 15, 1256 (1978).
[26]C. B. Duke, R. J. Meyer, A. Paton, J. L. Yeh, J. C. Tsang, A. Kahn, and P. Mark, J. Vac. Sci. Technol. 17, 501 (1980).
[27]R. J. Meyer, C. B. Duke, A. Paton, J. L. Yeh, J. C. Tsang, A. Kahn, and P. Mark (unpublished).
[28]D. J. Chadi (private communication).
[29]R. W. G. Wyckoff, *Crystal Structures* (Wiley, New York, 1963), Vol. I, pp. 108–111.
[30]C. B. Duke and C. W. Tucker, Jr., Surf. Sci. 15, 231 (1969).
[31]C. B. Duke, N. O. Lipari, and U. Landman, Phys. Rev. B 8, 2454 (1973).
[32]J. C. Slater, Phys. Rev. 81, 385 (1951).
[33]A. Kahn, E. So, P. Mark, R. J. Meyer, and C. B. Duke (unpublished).
[34]E. So, Ph.D. thesis, Princeton University, 1979 (unpublished).
[35]J. C. Phillips, Rev. Mod. Phys. 42, 317 (1970).
[36]S. V. Adhyapak and A. S. Niqavekor, J. Phys. Chem. Solids, 37, 1037 (1976).
[37]F. W. Lytle, Adv. x-ray Anal. 9, 398 (1966).
[38]C. B. Duke and A. R. Lubinsky, Surf. Sci., 50, 605 (1975).
[39]A. R. Lubinsky, C. B. Duke, S. C. Chang, B. W. Lee, and P. Mark, J. Vac. Sci. Technol. 13, 189 (1976).
[40]C. B. Duke, A. R. Lubinsky, S. C. Chang, B. W. Lee, and P. Mark, Phys. Rev. B 15, 4865 (1977).
[41]C. B. Duke, R. J. Meyer, A. Paton, and P. Mark, Phys. Rev. B 18, 4225 (1978).